INL EXT-21-63147

Initial Developments in Modeling Graphite Behavior

June 2021

Joseph Bass

Idaho National Laboratory

INL is a U.S. Department of Energy National Laboratory
operated by Batelle Energy Alliance, LLC

INL EXT-21-63147

Initial Developments in Modeling Graphite Behavior

Joseph Bass

June 2021

Idaho National Laboratory
Advanced Reactor Technologies
Idaho Falls, Idaho 83415

http://www.ART.INL.gov

Prepared for the
U.S. Department of Energy
Office of Nuclear Energy
Under DOE Idaho Operations Office
Contract DE-AC07-05ID14517

Page intentionally left blank

INL ART Program

Initial Developments in Modeling Graphite Behavior

INL EXT-21-63147

June 2021

Technical Reviewer: (Confirmation of mathematical accuracy, and correctness of data and appropriateness of assumptions.)

	22 June 2021
William Windes INL ART Graphite R&D Technical Lead	Date

Approved by:

M. Davenport	**6/22/2021**
Michael E. Davenport INL ART Project Manager	Date
Travis Mitchell	6/22/2021
Travis R. Mitchell INL ART Program Manager	Date
Michelle Sharp	6/22/2021
Michelle T. Sharp INL Quality Assurance	Date

Page intentionally left blank

ABSTRACT

In high-temperature reactor (HTR) designs, graphite is used as a moderator, reflector, and core material responsible for protecting the fuel and maintaining structural stability. From a safety perspective, it is imperative to predict how graphite will behave under reactor operating conditions that may compromise the core's structural integrity or the fuel's safety performance. The following report summarizes recent modeling work undertaken at Idaho National Laboratory (INL) focusing on graphite degradation behavior. One phenomenon that is explored in this report and can cause significant degradation to graphite properties is oxidation. Oxidation behavior in graphite is highly temperature dependent. At low temperatures, oxygen can fully penetrate a component and cause a homogeneous damage profile. At high temperatures, only the graphite near the surface of a component is affected. Understanding and modeling this temperature dependence is essential for predicting graphite behavior.

In this report, three graphite models are discussed. The first is used to investigate strength loss after low-temperature oxidation. It does this by generating an approximate graphite microstructure, then determining the required load to cause crack propagation. The model has been shown to reproduce the quasi-brittle stress-vs.-strain relationship observed in graphite. Strength loss results from the model are shown to match experimental values. The second model investigates strength loss under high-temperature oxidation conditions. This model is more applicable to full-scale graphite components, for which the oxidation damage is often inhomogeneous throughout. The third model computes stresses in graphite under reactor conditions. Specifically, the model incorporates the effect of creep, irradiation dose, thermal strains, and oxidation in order to predict component internal stresses. All these models are implemented in the Multiphysics Object-Oriented Simulation Environment (MOOSE), an open-source, parallel finite element framework.

Page intentionally left blank

CONTENTS

FIGURES

TABLES

Page intentionally left blank

ACRONYMS

ASME	American Society of Mechanical Engineers
HTR	high-temperature reactor
INL	Idaho National Laboratory
MOOSE	Multiphysics Object-Oriented Simulation Environment
POF	probability of failure
RVE	representative volume element

Page intentionally left blank

Initial Developments in Modeling Graphite Behavior

1. INTRODUCTION

In both new and existing high-temperature reactor (HTR) designs, the graphite within a graphite-core nuclear reactor acts as the core structural component, nuclear fuel container, neutron moderator, reflector, and thermal energy heat sink. To ensure safe operation of these reactors, the behavior of the graphite components must be well understood in terms of both normal and off-normal operating conditions. Potential issues during normal operations include irradiation-induced material property changes, a buildup of irradiation-induced internal stresses within the graphite microstructure, thermally induced stresses, and chronic oxidation leading to component structural failure. Off-normal events may create acute issues such as excessive thermally induced stresses, leading to component failure and rapid graphite oxidation before ultimately resulting in premature fuel failure. To protect the fuel and ensure the core's structural integrity, all these potential degradation issues must be evaluated to assess how the graphite is impacted.

The Advanced Reactor Technology R&D program has several activities empirically measuring these important degradation mechanisms. However, testing and property measurements regarding these degradation issues are necessarily limited (i.e., testing consists of small sample sizes that do not correspond with the expected large component sizes in a reactor).

American Society of Mechanical Engineers (ASME) Boiler and Pressure Vessel Code Section III, Division 5 addresses design rules for high-temperature nuclear materials intended for use within HTR designs. In Subsection HH, Subpart A, the code specifically addresses graphite, and outlines three methods for qualifying a graphite component for use in a nuclear reactor. The first two methods require computational modeling to ensure a sufficiently low probability of failure (POF), while the final method requires experimental testing of the component. In many cases, experimental testing of a graphite component may be prohibitively expensive or impractical, leaving modeling as the only way to fully qualify a component. Therefore, developing and implementing models capable of predicting graphite behavior is essential for both assessing degradation in existing reactors as well as qualifying components in novel designs.

This report will give a brief background on graphite oxidation, then cover three graphite models currently under development at Idaho National Laboratory (INL). The first, covered in Section 2.1, investigates strength loss from homogeneous oxidation at the microstructural level. The second, discussed in Section 2.2, investigates crack propagation in full-scale graphite components. The final model, discussed in Section 3.1, investigates stresses in graphite components subjected to a reactor environment.

2. GRAPHITE OXIDATION

Graphite is comprised almost entirely of carbon, which exothermically reacts with oxygen to create carbon monoxide and carbon dioxide. Removal of carbon atoms from the graphite crystal structure via oxidation can cause significant degradation to the graphite's properties, and thus is an essential consideration when assessing degradation in a graphite core component. A multitude of experimental work and modeling efforts have been conducted to determine the effect of oxidation on graphite [1,2,3,4]. Note that dozens of graphite oxidation studies have been carried out and published, and the cited references are in no way inclusive of all the work performed. However, even with the extensive work done to characterize graphite oxidation, significant knowledge gaps remain. This is partly due to the fact that no two grades of graphite behave exactly alike, necessitating that each grade be assessed individually. Other knowledge gaps are due to experimental limitations. One of the most prominent limitations of experimental work relates to the use of small specimens. Graphite core components can be larger than 1 m in some dimensions, and not all behavior that would occur in a large component can be captured in a small specimen. This is evident in graphite oxidation work in which the damage profile can be quite wide, depending on the testing conditions. These wide damage profiles cannot be fully captured in small

specimens, meaning that the graphite behavior associated with these wide profiles is not easily measured experimentally. Modeling, on the other hand, does not include a size limitation or issues involving the implementation of a wide oxidation profile.

Obtaining useful results for graphite oxidation relies in part on understanding oxidation's underlaying mechanisms. The main two mechanisms controlling graphite oxidation are oxygen gas diffusion and reaction kinetics. In a graphite crystallite, the reaction between carbon and oxygen only occurs at the ends of the graphene planes. These regions are termed "reactive surface areas," and their density varies depending on the grade of graphite. Correspondingly, if the diffusivity of oxygen through the graphite is high, more reactive surface areas will be available to react with oxygen, and a higher reaction rate can occur. Alternatively, if the diffusivity is slow, oxidation will only occur on the graphite surface. These behaviors can be seen experimentally. In low-temperature graphite oxidation experiments, the diffusivity is high relative to the reaction kinetics, causing oxygen to diffuse deep into the component and cause homogeneous oxidation damage throughout. At high temperatures, the reaction kinetics are high relative to the diffusivity, and the oxidation profile is primarily limited to the graphite surface. This temperature-dependent spatial variation in oxidation damage directly affects the graphite behavior [1]. For a more in-depth discussion on graphite oxidation mechanisms and microstructural development, interested readers are referred to the work of Kane [5,6] and Contescu [7,8]. ASTM standard D7542-15 [9] is also quite informative, as it covers a method for collecting graphite oxidation data and determining the transition from kinetically controlled (low temperature) to diffusion-controlled (high temperature) regimes.

In a reactor environment, oxidation can occur due to the trace amounts of oxygen inevitably present, or it can occur in an accident scenario in which a significant amount of oxygen enters the reactor. In either case, oxidation causes significant changes to the properties of graphite and must therefore be considered when designing components.

2.1 Oxidation Modeling: Microstructural Model

2.1.1 Microstructural Oxidation Model Introduction

A microstructurally based model was developed to study the effect of oxidation on the mechanical strength of a homogeneously oxidized component. This damage profile would be present in graphite oxidized at low temperature. The goal of the model is to reproduce the quasi-brittle stress-vs.-strain behavior seen in tensile testing of graphite. The model accomplishes this by approximating the graphite microstructure, then applying a load and simulating crack formation. To model crack formation, the model uses a phase-field fracture framework developed by Miehe [10] and built upon by Wu [11].

2.1.2 Phase-Field Fracture Numerical Model

The crack evolution in the system is characterized by a damage phase, *c*, which ranges from zero to one, with zero representing an undamaged region and one a fully damaged region. The transition from zero to one happens monotonically, as any decrease in the damage phase would correspond to the material healing. In crack modeling, explicit handling of a sharp crack topology is something to be avoided whenever possible. In this formulation, the crack is geometrically regularized through the use of the damage phase and its gradient. The regularized crack surface, A_S, takes the following functional form:

$$A_s = \int_\Omega \gamma(c, \nabla c)\, d\Omega \tag{1}$$

where Ω is the spatial domain and γ is the crack surface density. The functional form of the crack surface density is:

$$\gamma(c, \nabla c) = \frac{1}{2}\left(\frac{c^2}{l_0} + l_0 |\nabla c|^2\right) \tag{2}$$

where l_0 is an internal length parameter. This internal length helps to define the shape of the damage phase. The power balance in the system takes the following form:

$$P = \dot{E}_{dis} + \dot{E}_{stor} \tag{3}$$

where P is the power supplied by external loads, E_{dis} is an energy dissipated by crack formation, and E_{stor} is the strain energy. The energy dissipation rate from crack formation can be expressed as:

$$\dot{E}_{dis} = \int_{\Omega} g_c \dot{\gamma} \; d\Omega \tag{4}$$

where g_c is the energy release rate with units of energy per area. From a physical perspective, g_c is used to compute the energy dissipation caused by the crack evolution. By implementing a strain spectral decomposition, the total stored energy in the system is expressed as:

$$E_{stor} = \int_{\Omega} \Psi \; d\Omega \; = \; \int_{\Omega} (\omega(c) \, \Psi^{+} + \Psi^{-}) \, d\Omega \tag{5}$$

where Ψ is the elastic energy density, Ψ+ is the strain energy density associated with tensile stress, Ψ− is the strain energy density associated with compressive stress, and ω(c) is an energy-degradation function. The energy-degradation function monotonically transitions from one to zero as a function of the damage phase. Functionally, this precludes any tensile stress in a cracked region. The energy degradation function takes the following functional form:

$$\omega(c) = (1 - c)^2 \tag{6}$$

and the strain energy is expressed as:

$$\Psi^{\pm} = \frac{\lambda \langle \epsilon_1 + \epsilon_2 + \epsilon_3 \rangle_{\pm}^2}{2} + \mu \left(\langle \epsilon_1 \rangle_{\pm}^2 + \langle \epsilon_2 \rangle_{\pm}^2 + \langle \epsilon_3 \rangle_{\pm}^2 \right) \tag{7}$$

where λ is Lame's constant, ϵ_i is the i^{th} eigenvalue of the strain tensor, μ is the shear modulus, and $\langle \rangle_{\pm}$ is an operator that provides the positive or negative components by $\langle a \rangle_{\pm} = .5(a \pm |a|)$. The stress relation can be derived from the variation of the strain energy as:

$$\sigma = \frac{\partial \Psi}{\partial \epsilon} = \omega(c) \frac{\partial \Psi^{+}}{\partial \epsilon} + \frac{\partial \Psi^{-}}{\partial \epsilon} = \omega(c) \sigma^{+} + \sigma^{-} \tag{8}$$

where

$$\sigma^{\pm} = \frac{\partial \Psi^{\pm}}{\partial \epsilon} = \sum_{a=1}^{3} (\lambda \langle \epsilon_1 + \epsilon_2 + \epsilon_3 \rangle_{\pm} + 2\mu \langle \epsilon_a \rangle_{\pm}) \mathbf{n}_a \otimes \mathbf{n}_a \tag{9}$$

Here, n_a is the a^{th} eigenvector of the strain tensor. Ultimately, the stress is expressed as:

$$\sigma = [(1 - c)^2 (1 - k) + k] \sigma^{+} - \sigma^{-} \tag{10}$$

where k is a small positive number that ensures appropriate convergence behavior in the system. To ensure a monotonic increase in the damage phase and eliminate crack healing, a history variable, H, is introduced:

$$\Psi^{+} = H = \max_{t} (\Psi^{+}, 0) \tag{11}$$

Here, "$\max_{t}$" returns the max values over the simulation runtime. Ultimately, the damage phase evolution can be express as:

$$\dot{c} = -L \left(\frac{\delta E_{store}}{\delta c} + \frac{\delta E_{dis}}{\delta c} \right) = -L (2H(1 - c) + \Psi^{-} + \frac{2c \, g_c}{l_0} + \nabla g_c \, l_0 \cdot \nabla c \tag{12}$$

where L is the damage-phase mobility. This functional form of the damage-phase-field follows the Allen-Cahn equation, allowing for simplified implementation in the Multiphysics Object-Oriented Simulation Environment (MOOSE) framework.

2.1.3 Microstructural Oxidation Model Example Problem

To simulate a graphite's strength, an approximate microstructure must be generated. The true microstructure of graphite is quite complex and highly dependent on the fabrication process as well as the material used during fabrication [12]. Attempting to incorporate all microstructural features found in a particular grade of graphite is infeasible for this initial model development. In this work, emphasis is put on incorporating a representative pore structure typically found in most nuclear graphite grades. The pore structure plays a significant role in the quasi-brittle fracture behavior seen in graphite, with the pore edges experiencing high stresses and the pore itself acts as a low-energy pathway for crack propagation.

In this study, an approximated as-manufactured pore structure was generated based on the pore area and pore eccentricity distributions determined experimentally by Kane [13]. In these two-dimensional simulations, the pores are approximated by ellipses. Three examples of the approximated as-manufactured microstructure of graphite grade IG-110 are shown in the top row of Figure 1. They were generated by randomly positioning the elliptical pores featuring the experimentally determined area and eccentricity distributions. In this figure, light gray corresponds to graphite, and darker gray corresponds to the pores. Along with the as-manufactured pore structure, an oxidized pore structure was also generated. To approximate the uniformly oxidized pore structure expected for low-temperature oxidation, the major and minor axes of the elliptical pores are simply enlarged. This pore enlargement procedure, used to approximate oxidation, is based primarily on the following two assumptions: (1) oxygen is homogeneously distributed throughout the graphite and is at sufficiently high partial pressure so as to not be rate limiting, and (2) all pore surfaces are oxidized more or less equally. In the second and third rows of Figure 1, examples of the approximated pore structures corresponding to 5 and 10% mass loss, respectively, are shown. Moving forward, a microstructural approximation (e.g., the nine shown in Figure 1) will be referred to as a "representative volume element" (RVE).

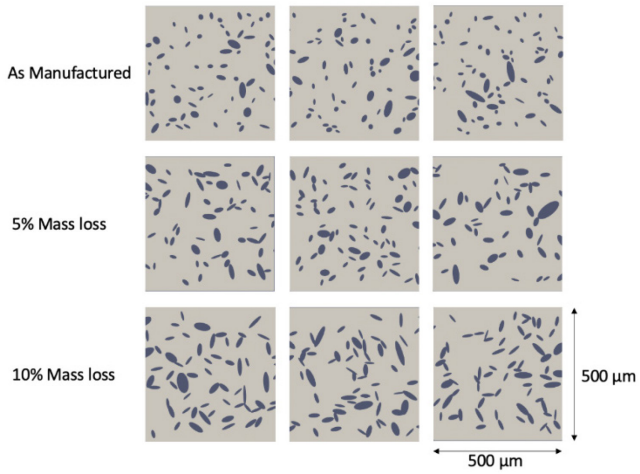

Figure 1. Approximated pore structures of as-manufactured and oxidized IG-110.

To determine the strength of a particular RVE, the bottom of the RVE is fixed, and a velocity is applied to the top boundary. This procedure is intended to reproduce conditions that occur during a tensile test, and a schematic of the procedure is shown on the left in Figure 2. The resultant damage phase at the end of the simulation is shown on the right in Figure 2.

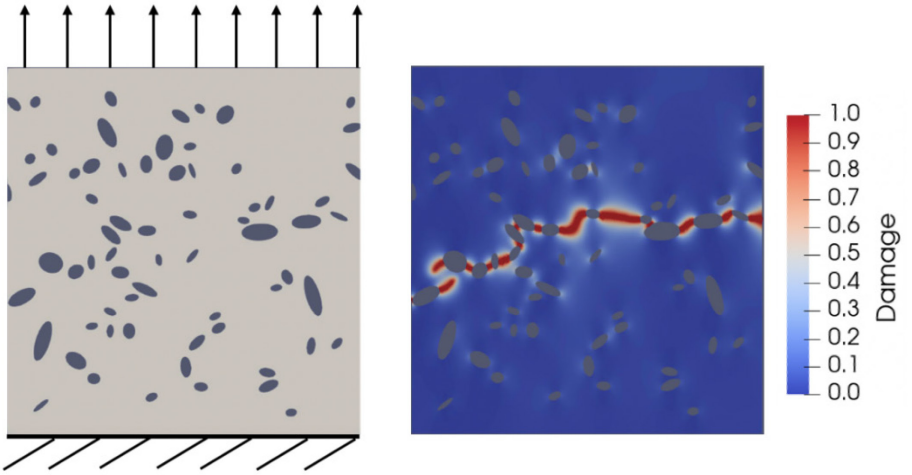

Figure 2. Tensile loading schematic (left) and resultant damage phase (right).

The results from an example simulation of an as-manufactured microstructure are shown in Figure 3. The evolution of the damage phase at various times during the simulation is shown in the images labeled A–D, and the computed stress-vs.-strain is shown in the plot on the right. A, B, C, and D on the left side of Figure 3 correspond to A, B, C, and D in the stress-vs.-strain curve. From Figure 3, we can see an approximately linear stress-strain relationship between A and B. At C, the formation of the first cracks causes a drop in stress. Between C and D, multiple cracks form, and maximum stress is reached at around 20 MPa. In the plot, a quasi-brittle stress-strain relationship is apparent, due to the smooth curvature near the maximum stress. This is the expected behavior based on experimental results.

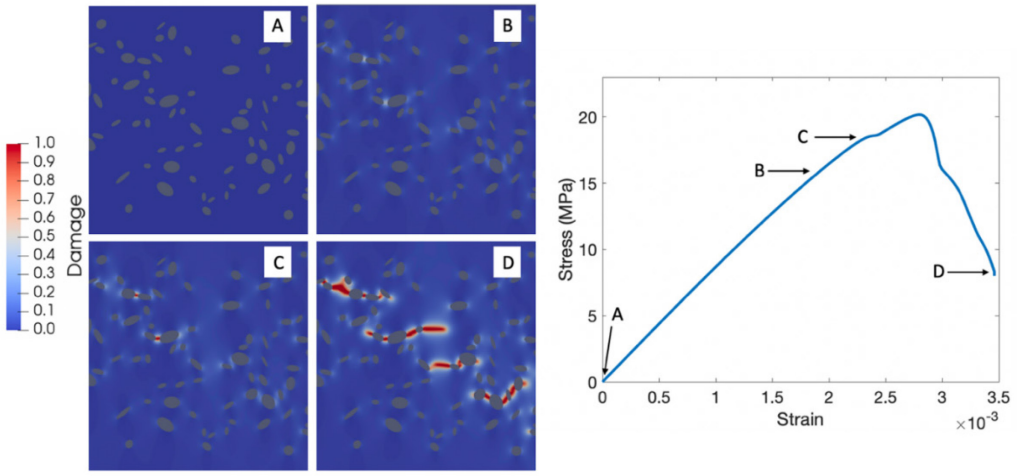

Figure 3. Damage phase evolution in an RVE (left) and corresponding stress-vs.-strain plot (right).

2.1.4 Microstructural Oxidation Model: Results and Discussion

Seventy RVEs were generated for the as-manufactured, 5% mass loss, and 10% mass loss cases, for a total of 210 RVEs. Note that each RVE is distinct, since the pores are randomly generated from the experimental distributions and then randomly positioned. Each of these RVEs was subjected to the tensile procedure discussed above, and the maximum stress was recorded. Table 1 presents a statistical breakdown of the maximum stress distribution for the as-manufactured, 5% mass loss, and 10% mass loss cases. From this table, the model is shown to predict a strength of 22.25 MPa, which is in reasonable agreement with the 25.69 MPa experimental value. The difference between these values may be the result

of several factors. One source of error could be due to the simplified microstructure used in this model. It is possible that elliptical pores are not truly sufficient to represent the microstructure, and a more complex microstructure would yield improved results. This is particularly pertinent for the oxidized microstructural approximation. Experiments have shown that the binder phase of graphite will often oxidize before the filler particles. Thus, differentiating filler particles from binder material may generate additional insights not provided by the current microstructural approximation. Another source of error could be that the model's parameterization does not accurately capture the graphite behavior. Lower scale effects such as microcracking are not explicitly incorporated into the model; instead, the lower scale behavior is accounted for via the model's parameterization. It is difficult to verify how well the parameterization accounts for these lower scale effects. Regarding the standard deviation, the model predicts a slightly larger value than that found in the experimental data. This difference may be partly due to size effects. For multiple grades of graphite, it was shown that, as specimen size decreases, the variability in the measured property increases [15]. In this case, the simulations consider a smaller specimen than the experiments [14], so the larger variance in the simulation results is unsurprising.

Table 1. Experimental and simulated tensile strength distribution in IG-110.

	Mean	Standard Deviation	Scale	Shape	Ref
As-Manufactured Experimental	25.69	1.88	25.51	16.19	[14]
As-Manufactured Simulated	22.25	2.34	23.26	11.51	
5% Mass Loss Simulated	15.45	1.78	16.21	10.49	
10% Mass Loss Simulated	9.96	1.64	10.63	7.14	

The percent strength loss is computed as:

$$strength\ loss\ = \frac{\sigma_1 - \sigma_2}{\sigma_1} \tag{13}$$

where σ_1 is the as-manufactured maximum stress and σ_2 is the maximum stress after oxidation. Table 2 shows the simulated percent strength loss as well as the percent strength loss determined from upsetting experiments.

Table 2. Simulated and experimental strength loss from oxidation.

	5% mass loss	10% mass loss
Simulation	30.5%	55.2%
Experiment	33.0%	53.0%

In comparing the simulated and experimental numbers, they are shown to match very well. Based on these results, it is apparent that the model can reproduce the strength loss behavior observed experimentally in the as-manufactured and oxidized IG-110. This supports the model's implicit assumption that the large pores in the pore structure are a primary contributor to the observed strength and crack behavior. Future directions for this work could consider incorporating a more complex microstructural approximation or additional grades of graphite. IG-110 is a super-fine grain grade, so parameterizing this model for a graphite with a larger grain size could provide insights into the model's applicability for all grades.

2.2 Oxidation Modeling: Full-Scale Model

2.2.1 Full-Scale Oxidation Model: Introduction

The full-scale model seeks to investigate strength loss due to oxidation in an inhomogeneously oxidized component. In the microstructural model discussed in the previous section, the oxidation was assumed to be homogeneous. This will not be the case in a full-scale graphite component, unless the graphite is at low temperature (in which case the diffusivity is much higher than the reaction kinetics), In general, graphite at reactor temperatures displays neither homogeneous oxidation nor oxidation only on the surface. Instead, a smooth oxidation damage profile will be generated within the component, and the local properties will be a function of the local oxidation damage. Experiments have shown that variations in oxidation profiles can cause significant variation in graphite behavior [1]. Thus, to model strength loss in a full-scale component, a model must account for inhomogeneous oxidation damage and estimate the oxidation damage profile.

The full-scale model developed in this work is built on the same phase-field fracture formulation outlined in Section 2.1.2. Conceptually, the full-scale model no longer considers the graphite at a microstructural level, so no pores are explicitly incorporated into the mesh. Instead, the local properties are set based on the local oxidation damage. One implicit assumption in this model is that the local properties within the component can be described as a function of oxidation mass loss. Low-temperature experiments such as those being performed at INL can be used to determine these mass-loss-dependent properties. The inputs required by the model are the density profile caused by oxidation, the properties of the graphite as a function of density, and the component geometry.

2.2.2 Full-Scale Oxidation Model: Example Problem

For a simple example problem, we consider a block of graphite with an oxygen concentration being applied to its right side, as shown in Figure 4. A graphite oxidation model previously developed at INL by Kane [5] is used to compute density profiles in oxidized graphite. This model can produce spatially and temporally resolved mass loss profiles in graphite, based on grade-specific parameters, temperature, and component geometry. This graphite oxidation model has proven to be able to reproduce experimental results.

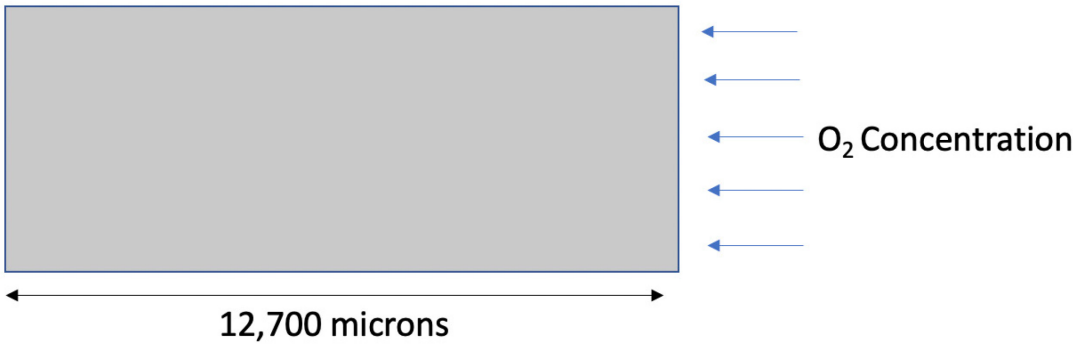

Figure 4. Example oxidation problem setup.

A high- and a low-temperature simulation were run using the setup shown in Figure 4. Doing so enabled the generation of two distinct density profiles. These normalized density profiles from oxidation in IG-110 occurring at 500 and 700°C are presented in Figure 5. The simulations for both temperatures are run to 10% mass loss. At 500°C, the temperature is low enough to produce a homogeneous oxidation profile, while at 700°C, the oxidation profile is inhomogeneous. Based on these profiles, a crack is expected to initiate at a random location in the block oxidized at 500°C, whereas a crack is expected to initiate on the right side of the block oxidized at 700°C.

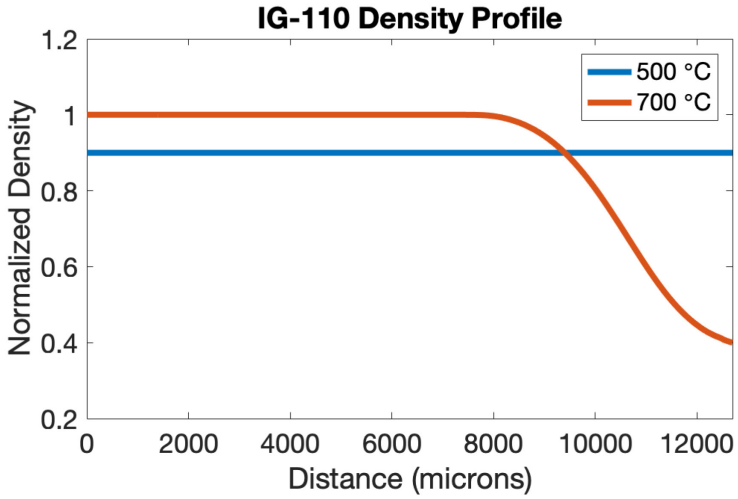

Figure 5. Simulated density profiles for G-110 at 500 and 700°C.

Apart from the block's density profile (Figure 5), the full-scale model requires density-dependent properties. Many of these properties are being determined experimentally at INL and should be available in upcoming publications. One of the parameters needed in this model is the local fracture strength. Results from the microstructurally based oxidation model discussed in the previous section provide mass-loss-dependent fracture strength distributions (Table 1). These strength distributions for the as-manufactured, 5% mass loss, and 10% mass loss states are plotted in Figure 6.

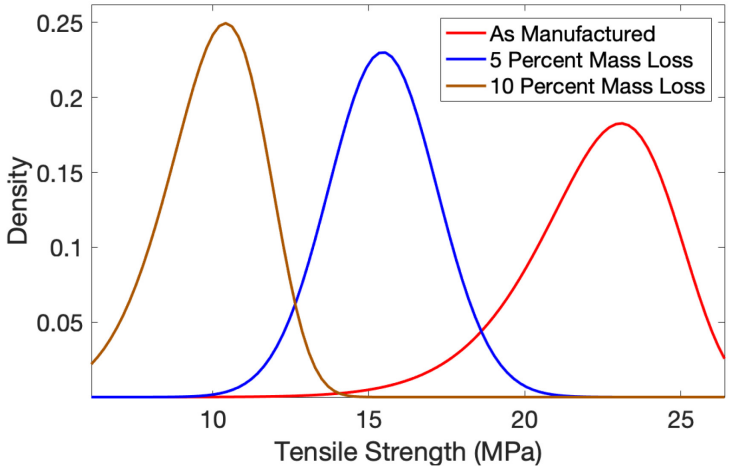

Figure 6. Computed Weibull distributions for the strength of IG-110 at multiple levels of mass loss.

The graphite blocks are assigned density-dependent properties, based on the density profiles shown in Figure 5 as well as the property distributions. During a simulation, the bottom boundary of the block is fixed, and the top is raised to apply a tensile load. Preliminary results of the crack evolution for the 500°C block and 700°C blocks are shown in Figures 7 and 8, respectively. In these figures, the images labeled 1 shows the crack initiation, and images labeled 2–4 reveal the propagation of the crack throughout the simulation. In Figure 7, the crack does appear to initiate at a random location and propagate both to the left and the right. As for Figure 8, the crack initiates on the right side (where more oxidation has occurred) and progresses inward. Thus, the expected crack initiation and propagation behavior is produced.

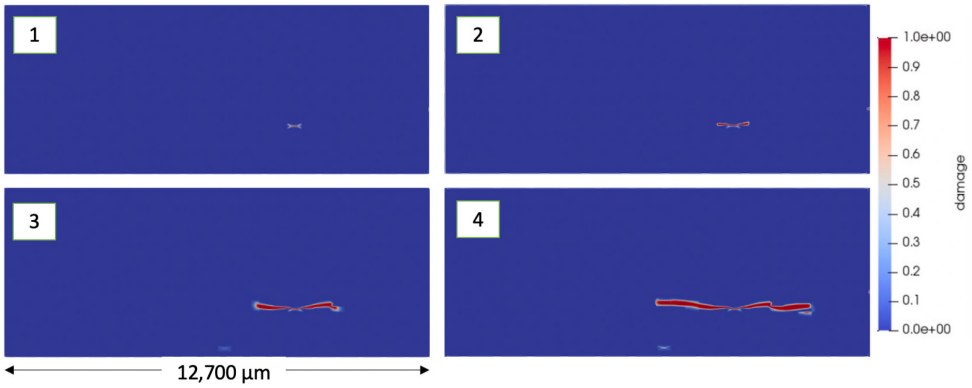

Figure 7. Crack propagation in an IG-110 block oxidized at 500°C at 10% mass loss.

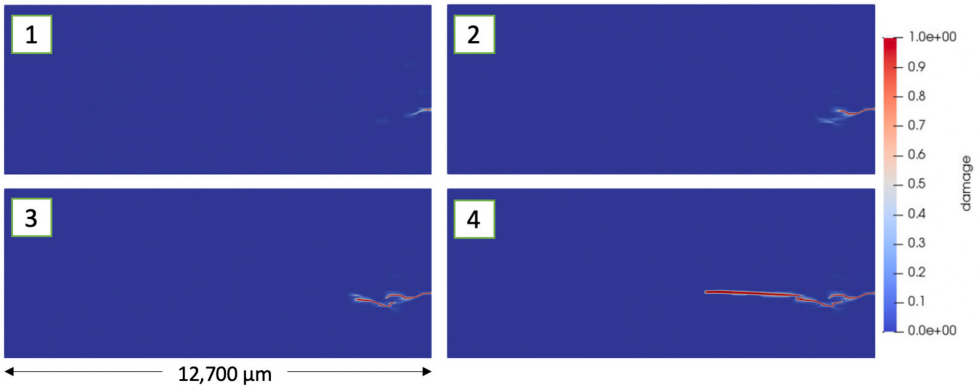

Figure 8. Crack propagation in an IG-110 block oxidized at 700°C at 10% mass loss.

2.2.3 Full-Scale Model: Results and Discussion

The computed tensile strength in these preliminary simulations for the 500 and 700°C cases is approximately 7 and 3 MPa, respectively. These values are below the expected range. Matthews found that, for IG-110 oxidized to 10% mass loss at 550 and 750°C, there was a compression strength decrease of approximately 50 and 20%, respectively [1]. If we assume IG-110 has an unoxidized tensile strength of 25 MPa, and that the strength loss ratio for tensile tests is similar to that for compressive tests, the simulated 500 and 700°C cases should have a tensile strength of around 12.5 and 20 MPa, respectively.

Analysis of these simulations reveals that, once a crack initiates, it propagates through the entire block. If we consider the block oxidized at 700°C, severe oxidation damage is seen on the right-hand side. This means cracks will initiate at low stresses in this region, and ultimately cause the block to fail at these low stresses. No region of the 500°C block is as damaged as the 700°C block; thus, cracks do not initiate until higher stresses are achieved. In a physical graphite component, cracks that form in weak areas can propagate into pores or other defects, and do not necessarily cause unstable crack propagation. Additional work is currently underway to investigate and resolve the cause of this low-stress fracture behavior.

3. GRAPHITE INTERNAL STRESS MODELING

According to the ASME Boiler and Pressure Vessel Code, to qualify a graphite component without full-scale experimental testing, the internal stresses must be computed in order to be used with the Simple or Full Assessment methodologies. Recent modeling efforts have focused on developing a model within MOOSE that will be capable of modeling the internal stresses that may occur in a reactor environment. The model is intended to account for temperature variation, oxidation, and irradiation effects within graphite components.

3.1 Internal Stress Modeling

3.1.1 Internal Stress Modeling: Introduction

Previous work on modeling internal stresses in graphite often considered a total strain comprised of an elastic strain component, a thermal strain component, an irradiation-induced strain component, and a creep strain component. This approach will be continued in this work. In a real system, most of these strain components are highly dependent on the dose, temperature, and oxidation experienced by the graphite. A group at Argonne National Laboratory recently finished developing a model in MOOSE that considers dose- and temperature-dependent stress generation in graphite [16]. Their work is an ideal starting point for this study. However, a primary aspect that needs to be added to their model is the effect of oxidation on the material properties.

To parameterize the model, the following are needed: the thermal conductivity, coefficient of thermal expansion, Young's modulus, Poisson's ratio, primary and secondary creep coefficients, and irradiation-induced eigenstrain relationship. Note that, for anisotropic graphite, these parameters are needed in all directions. Also, these properties and relationships may be a function of dose, temperature, density (oxidation), or a combination of all three.

3.1.2 Internal Stress Modeling: Example Simulation

To run example simulations, a component geomerty was taken from part of a partial prismatic core fuel block design [17]. This geometry is shown in Figure 9.

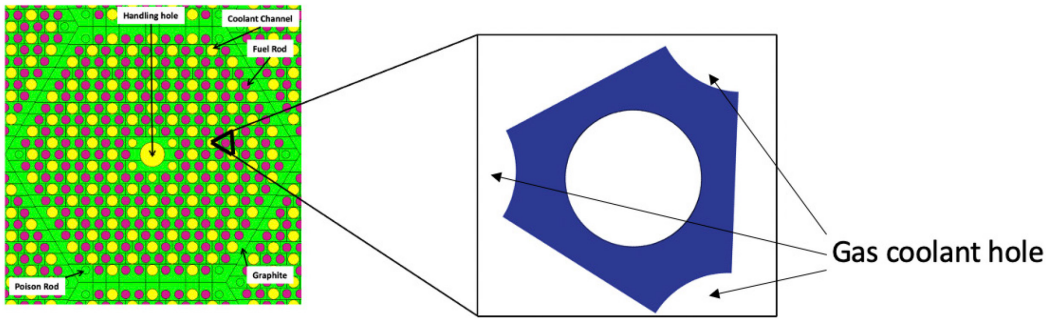

Figure 9. Prismatic fuel (left [17]) and the component geometry used in example simulations (right).

The model was parameterized primarily from experimental data available in the International Atomic Energy Agency's graphite database. Parameter surfaces were fit using MATLAB. Preliminary example parameter fits for graphite Pile Grade A (PGA) are shown in Figure 10.

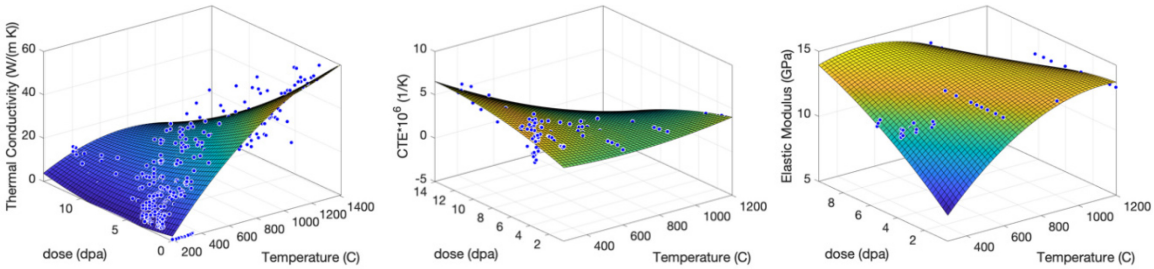

Figure 10. Example parameter surface fits of graphite properties.

Using these parameter fits, a simulation was initiated that imposes an irradiation dose that increases over time. The neutron dose profile at 10,000 hours is shown in the left-hand image in Figure 11. A temperature boundary condition fixes the gas holes and center hole temperatures at 600 and 700°C,

respectively. The resultant stress distribution is generated by a variation in thermal expansion caused by the temperature gradient, as well as irradiation-included swelling and irradiation creep. The stress is shown on the right in Figure 11. A preliminary check of the stresses produced during this simulation are well within a reasonable range.

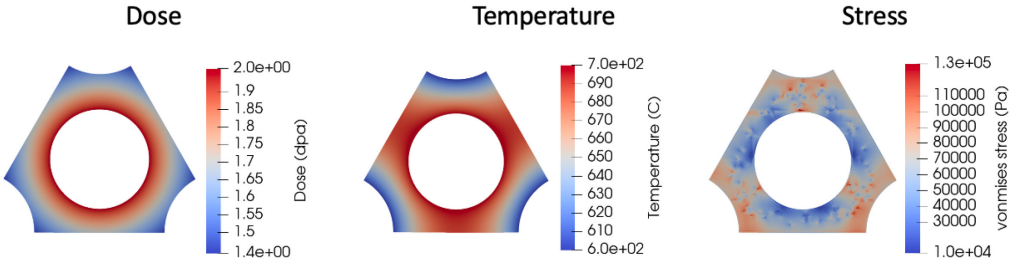

Figure 11. Irradiation dose (left), temperature (center), and resultant stress (right) in an example simulation.

To model stresses generated after a graphite component has been oxidized, the model must implement the properties as a function of mass loss. Oxidation simulations were run to determine density profiles in the components at high and low temperatures. The low-temperature simulation implemented a gas temperature of 500°C and a center hole temperature of 550°C. The high-temperature simulation sets the gas coolant temperature at 600°C and the center hole temperature at 650°C. These temperature profiles are shown in the left column of Figure 12. A preliminary simulation was run that incorporated density-dependent properties based on density profiles generated using Kane's oxidation model. These density profiles for both high and low oxidation temperatures are shown in the middle column of Figure 12. As seen in the figure, the higher temperature has a much narrower density profile compared to the lower temperature simulation. The generated stresses are shown in the right column of Figure 12. In general, although the thermal conductivity is affected by the mass loss, a significant temperature profile difference between the high- and low-temperature simulations was not observed. The stresses in the simulations are generated by the variation in thermal expansion caused by the temperature gradient. The difference between the computed stresses in high- and low-temperature oxidation simulations is insignificant. As expected, the main behavioral difference results from the reduced strength inflicted by the oxidation on the graphite component.

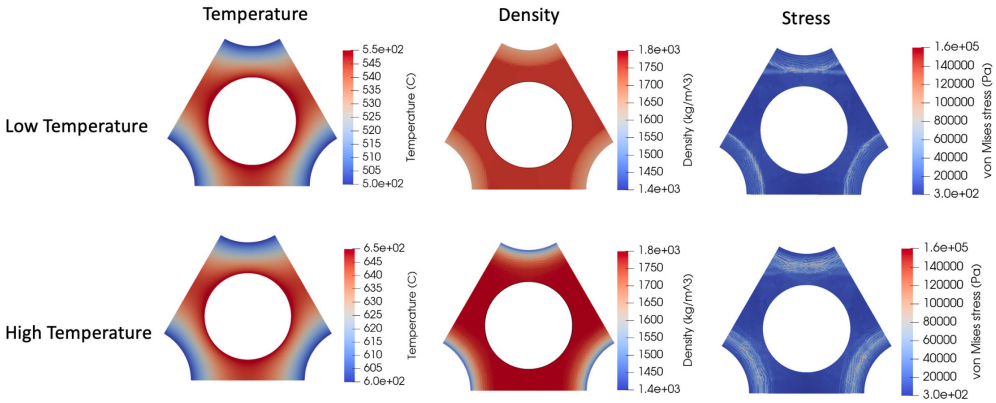

Figure 12. Temperature (left), density (center), and resultant stress (right) in an example simulation.

3.1.3 Internal Stress Modeling: Conclusions and Future Work

The internal stresses computed in the test problems seem very reasonable. Additional efforts are underway to better couple the oxidation model developed in Kane's work to the stress calculation. One additional topic for future work that is of particular interest is a validation study of this model against experimental or other computational results. It is also important to note that one purpose of this modeling effort is for use in conjunction with the ASME code to determine changes to the POF for a graphite core component during service in a nuclear application. Effectively incorporating oxidation effects into the POF calculation is currently being pursued by the ASME Nonmetallic Working Group. Future work will couple this model to the ASME code.

4. CONCLUSIONS

Modeling graphite behavior within a nuclear environment is essential for ensuring that a component remains reliable throughout its design life. A primary degradation mechanism identified for high-temperature gas reactor designs is oxidation of the components. This can occur either during normal operations with trace amounts of oxidant, or during acute accident conditions involving high temperatures and large oxidant levels. This report covered three graphite models being developed at INL. The first uses a phase-field fracture formulation alongside an approximated defect microstructure to predict how oxidation may affect the observed strength of homogeneously oxidized graphite. Results from this fracture model compare well with experiment. The second model investigates crack propagation and strength loss in an inhomogeneously oxidized large component. In this model, cracks are generated from phase-field fracture formulation, and the model is parameterized using results from the microstructurally based oxidation model and experiments being performed at INL. Appropriate density profiles are generated by a separate oxidation model and determine the local properties. While results from this full-scale model reproduce the expected qualitative behavior, the quantitative results demonstrate the model's need for additional refinement. The third model presented in this report computes internal stresses in a graphite component based on expected HTR conditions. Preliminary results from this model are reasonable in regard to both oxidized and irradiation conditions. However, as discussed, additional work is necessary to validate the model and couple it to the ASME code in order to compute the degraded component POF after service in a nuclear application.

5. REFERENCES

[1] Matthews, A., J. Kane, D. Swank, W. Windes, "The Degradation of Strength under Varying Oxidizing Conditions for Nuclear Graphite." INL/EXT-19-53723, 2019.

[2] Smith, R., "Status of Graphite Oxidation Work". INL/EXT-10-18880. May, 2010.

[3] Burchell, T., I. Pickup, B. McEnaney, R. Cooke. "The Relationship Between Microstructure and the Reduction of Elastic Modulus in Thermally and Radiolytically Corroded Nuclear Graphite" Carbon, Volume 24, No 5, 1986, pp. 545-549.

[4] Burchell, T., T. Yahr, R. Battiste, "Modeling the Multiaxial Strength of H-451 Nuclear Grade Graphite". Carbon, Volume 45, 2007, pp. 2570-2583.

[5] Kane, J., C. Contescu, R. Smith, G., Strydon, W. Windes, "Understanding the reaction of nuclear graphite with molecular oxygen: Kinetics, transport, and structural evolution". Journal of Nuclear Materials, Volume 493, 2017, pp. 343-367.

[6] Kane, J., A. Matthews, C. Orme, C. Contescu, W. Swank, W. Windes, "Effective gaseous diffusion coefficients of select ultra-fine, super-fine and medium grain nuclear graphite". Carbon, Volume 136, 2018, pp. 369-379.

[7] Contescu, C., R. Mee, Y. Lee, J. Arregui-Mena, N. Gallego, T. Burchell, J. Kane, W. Windes, "Beyond the classical kinetic model for chronic graphite oxidation by moisture in high temperature gas-cooled reactors". Carbon, Volume 127, 2018, pp. 158-169.

[8] Wang, P., C. Contescu, S. Yu, T. Burchell, "Pore structure development in oxidized IG-110 nuclear graphite". Journal of Nuclear Materials, Volume 430, 2012, pp. 229-238.

[9] ASTM International, "ASTM D7542-15 Standard Test Method for Air Oxidation of Carbon and Graphite in the Kinetic Regime".

[10] Miehe, C., L. Schanzel, H. Ulmer, "Phase-field modeling of fracture in multi-physics problems. Part I. Balance of crack surface and failure criteria for brittle crack propagation in thermo- elastic solids". Comput. Methods Appl. Mech. Engrg., Vol. 294, 2015, pp. 449-485.

[11] Wu, J., "A Unified Phase-field Theory for the Mechanics of Damage and Quasi-brittle Failure", Journal of the Mechanics and Physics of Solids, Vol. 103, 2017, pp. 72-99.

[12] Kyaw, S., W. Sun, A. Becker, "Effects of Composition of filler, binder and porosity on elastic and fracture properties of nuclear graphite". Journal of Nuclear Materials, Volume 457, 2015, pp. 42-47.

[13] Kane, J., C. Karthik, D. Butt, W. Windes, R. Ubic, "Microstructural characterization and pore structure analysis of nuclear graphite". Journal of Nuclear Material Vol. 415, 2011, pp. 189-197.

[14] Burchell, T., "A Microstructurally Based Fracture Model for Polygranular Graphites". Carbon, Volume 34, Number 3, 1996, pp. 297-316.

[15] Chi, S., "Specimen size effects on the compressive strength and Weibull modulus of nuclear graphite of different coke particle size: IG-110 and NBG-18". Journal of Nuclear Materials, Volume 436, 2013, pp. 185-190.

[16] Nicolas, A., M. Messner, T. Sham, "Preliminary design analysis workflow for Division 5 HHA-3200 requirements for graphite core components". Applied Materials Division Argonne National Laboratory. ANL-ART-197. August 2020.

[17] Sterbentz, J., P. Bayless, L. Nelson, H. Gougar, J. Kinsey, G. Strydon, "High Temperature Gas-Cooled Test Reactor Point Design: Summary Report". INL/EXT- 16-37661. March 2016.